

INITIAL-MODEL CONSTRUCTION FOR MVA TECHNIQUES

H. B. Santos, J. Schleicher and A. Novais

email: *hbuenos@gmail.com, js@ime.unicamp.br*

keywords: *Time-migration, migration velocity analysis, seismic velocity interpretation and processing*

ABSTRACT

For iterative migration-velocity-analysis (MVA) methods, good starting models are required. We discuss the parameterization of two recent time MVA methods, being common-image-gather image-wave propagation and double multi-stack migration, and compare their potential for the construction of initial models for more sophisticated MVA techniques. Both methods are able to generate a velocity model and a time-migrated image without a-priori information. While multi-stack MVA is already fully automatic by design, we eliminate human intervention from image-wave MVA by introducing automated picking of the involved flattening velocities. At the example of the Marmousoft dataset, we show that both methods can produce equivalent results at comparable cost.

INTRODUCTION

A major challenge both in seismic exploration and in seismological investigations is the construction of the best possible undistorted image in depth from the acquired data. For this purpose, imaging methods are employed that rely on the knowledge of a subsurface velocity model. Most present-day model-building techniques are iterative procedures that improve a starting model based on intermediate results. Among these, most important are model-building methods based directly on migration itself, so-called migration velocity analysis (MVA). All of these techniques strongly depend on the quality of the starting model.

Conventional techniques for constructing a starting model are methods based on an analysis of the traveltimes of seismic waves. Among the most commonly used methods are the Common-MidPoint (CMP) and Common Reflection Surface (CRS) stacks (see, e.g., Hertweck et al., 2007).

Both these methods operate in the data-acquisition time domain. Thus, there is a need for transforming such a velocity model to the migration domain, be it in time or depth. This conversion is problematic in that it depends on the actual values of the velocity model to be converted (Hubral, 1977). Therefore, alternative velocity-analysis methods are desirable that work directly in the desired migration domain, so that there is no need for a conversion of the model domain.

Motivated by the importance of the subject, MVA methods have been proposed by many authors. Because of its conceptual clarity and simplicity, residual moveout (RMO) analysis has become a favorite tool for MVA. In recent years, many improvements have been proposed. However, few authors have studied the problem of how to construct the best possible starting model. Schleicher et al. (2008) and Schleicher and Costa (2009) proposed two MVA methods for time migration that can fill this gap. The first one treats the events in common-image gathers (CIGs) similar to wavefronts and lets them propagate until they are flat, updating the migration velocity model from the flattening velocities (Schleicher et al., 2008). The second method stacks twice over migrated images for many models with different weights in order to extract stationary migration velocities from the ratio of the images (Schleicher and Costa, 2009). Both MVA methods' purpose is to begin the analysis from scratch, without the need to specify an initial velocity model that has already certain features of the searched model. Thus, they differ fundamentally from tomographic methods (Billette et al., 2003; Clapp et al., 2004) or full waveform inversion (FWI, see, e.g., Virieux and Operto, 2009), which require a good initial model to ensure convergence.

After application of an adequate time-to-depth conversion algorithm (Cameron et al., 2007, 2008; Iversen and Tygel, 2008), a high-quality time-migration initial model may even provide sufficient quality to serve for subsequent depth MVA or FWI methods.

Schleicher et al. (2008) and Schleicher and Costa (2009) tested their time-migration MVA methods on the synthetic Marmousoft dataset (Billette et al., 2003). These synthetic data were obtained by Born modeling in a smoothed version of the original Marmousoft model, using the original reflectivity. However, although these authors applied both methods to the same dataset, they did not compare their performance or try to combine them.

In this work, we deliver this comparison using the Marmousoft model, not only with respect to the quality of the resulting velocity models and migrated images, but also regarding the human and computational effort required to achieve a certain quality. Another goal of our research is to study the setting of the parameters involved in the methods, in order to optimize their performance. Parameter to be cited in this respect are the measure of nonflatness of the events in the common image gather (CIG) or the number of CIGs necessary for a successful analysis.

MVA TECHNIQUES

We start with a brief review of the migration-velocity-analysis techniques under consideration.

MVA by image-wave propagation of CIGs

Theoretical Description Schleicher et al. (2008) started from the position of a horizontal reflector below a homogeneous medium with constant-velocity v_m as a function of vertical time τ , half-offset h , and migration velocity v , as derived by Al-Yahya (1989). It reads

$$\tau = \sqrt{\tau_0^2 + h^2(1/v_m^2 - 1/v^2)}, \quad (1)$$

where τ_0 is vertical time at zero offset, i.e., the true migrated position of the reflector image. They arrived at the image-wave equation for the continuation of a CIG,

$$\frac{\partial \tilde{p}}{\partial \tau} + \frac{v^3 \tau}{h^2} \frac{\partial \tilde{p}}{\partial v} = 0. \quad (2)$$

Note that equation (2) does not depend on the medium velocity v_m nor the correct zero-offset vertical time τ_0 of the reflector. This equation was independently derived by Fomel (2003), who called it the kinematic RMO equation.

Schleicher and Biloti (2007) presented the equivalent of equation (1) for depth migration

$$z = \sqrt{\frac{v^2}{v_m^2} z_0^2 + \left(\frac{v^2}{v_m^2} - 1\right) h^2}, \quad (3)$$

where z_0 is the true depth of the supposedly horizontal reflector and z is the migrated pseudodepth.

Based on equation (3) and in analogy to the procedure in time, Schleicher et al. (2008) showed that the equation for continuation of the CIGs in depth can be written as

$$\frac{\partial p}{\partial z} + \frac{vz}{h^2 + z^2} \frac{\partial p}{\partial v} = 0. \quad (4)$$

Because of the initial hypothesis of a horizontal reflector, equations (2) and (4) do not describe a dislocation of the image along the half-offset axis. The complete equation for dipping reflectors, which includes a derivative with respect to h , can be found in Fomel (2003). However, since the dislocation in the h direction is the smaller the closer the model is to the true one, equations (2) and (4) are sufficient for an iterative procedure (see also Al-Yahya, 1989).

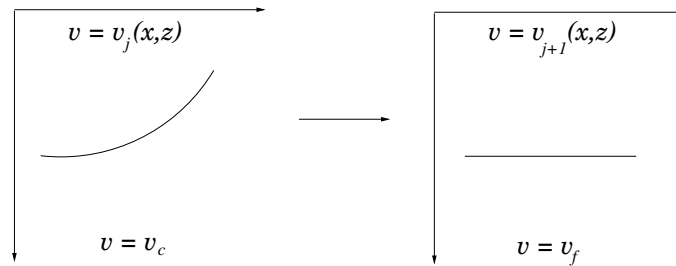


Figure 1: Iterative velocity model construction by image-wave propagation of CIGs. Here v_j represents the present velocity model at the j th iteration; v_{j+1} is the updated velocity model; v_c is the constant velocity to begin the image continuation (e.g., water velocity $v_0 = 1500$ m/s for marine data or near-surface velocity for land data); and v_f is the constant velocity that flattens an event.

Iterative model building For a velocity model construction using the continuation of a single CIG, Schleicher et al. (2008) proposed the following iterative procedure (Figure 1):

1. Migrate data with inhomogeneous velocity model v_j .
 2. Organize data into CIGs.
- If CIGs are not flat:
3. Let CIGs propagate as if obtained with constant velocity v_c .
 4. For each event, determine the flattening velocity v_f .
 5. Use v_f to update the velocity model v_j to v_{j+1} .
 6. Go to 1.

In this way, we are able to update the velocity model using the concepts of residual migration. Residual migration is based on the fact that migrating a time-migrated image a second time yields a time-migrated image as if directly obtained with an effective migration velocity (Rocca and Salvador, 1982). If the first migration uses velocity v_1 and the second migration velocity v_2 , then the effective migration velocity v_{ef} can be expressed as

$$v_{ef} = \sqrt{v_1^2 + v_2^2}. \quad (5)$$

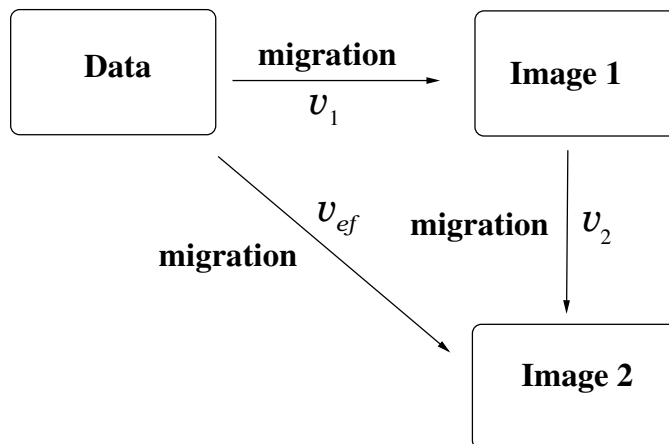


Figure 2: Pythagoras Theorem of Time Migration.

Equation (5) can be called to the Pythagoras Theorem of Time Migration as illustrated in Figure 2. Rewriting it as

$$v_2 = \sqrt{v_{ef}^2 - v_1^2}, \quad (6)$$

it allows to determine the necessary residual migration velocity v_2 that will transform an image after migration with velocity v_1 into an image for the desired effective migration velocity v_{ef} .

In our image continuation procedure, the initial image was obtained by migration with model v_j , which thus is our v_1 . The desired velocity model is the one where events are flat, hopefully achieved at the next iteration, i.e., $v_{j+1} = v_{ef}$. Thus, we need a residual velocity $v_2 = \sqrt{v_{j+1}^2 - v_j^2}$. On the other hand, we have treated the image as if migrated with v_c , which thus may also assume the role of v_1 in equation (6). The event is approximately flattened at v_f , which thus also represents v_{ef} , implying that the residual velocity should be approximated by $v_2 \approx \sqrt{v_f^2 - v_c^2}$. Equating these two expressions for the residual-migration velocity v_2 , the velocity updating formula reads (Schleicher et al., 2008)

$$v_{j+1} \approx \sqrt{v_j^2 + v_f^2 - v_c^2}. \quad (7)$$

This formula allows to obtain an updated velocity model (v_{j+1}) as a function of the present velocity model (v_j), the constant velocity that flattens an event (v_f) and the constant velocity used to start the image continuation (v_c). To avoid a so-called Derogowski loop with only local velocity improvements without achieving global convergence, the model should be smoothed between iterations.

MVA by double multi-stack migration

We compare the procedure and result of the above technique to the one of Schleicher and Costa (2009), which is based on the multipath-summation imaging process of Landa et al. (2006). The fundamental idea is to stack the migration results for “all possible” velocities, or at least as much models as practically reasonable. Since only “good” models yield flat events in common-image gathers, these will prevail in the overall stacked image, which thus will show the geologic structure without the need for a migration-velocity model. Below, we will refer to this technique as multi-stack migration.

Using the notation of Landa et al. (2006), the multi-stack time-migration operator by can be written as

$$V_W(\mathbf{x}) = \int d\alpha w(\mathbf{x}, \alpha) \int d\xi \int dt U(t, \xi) \delta(t - t_d(\xi, \mathbf{x}; \alpha)), \quad (8)$$

where V_W is the resulting time-migrated image at an image point with coordinates $\mathbf{x} = (x, \tau)$, x being the lateral distance, τ vertical time, $U(t, \xi)$ a seismic trace at coordinate ξ in the seismic data, $t_d(\xi, \mathbf{x}; \alpha)$ is a stacking surfaces corresponding to a set of possible velocity models that are parameterized using variable α and $w(\mathbf{x}, \alpha)$ is a weight function, which serves to attenuate contributions from unlikely trajectories and emphasize contributions from trajectories close to the optimal.

In the application of Schleicher and Costa (2009), α directly represented the time-migration velocity and the weight $w(\mathbf{x}, \alpha)$ was given by a bell-shaped exponential formula with peak value at zero dip in the common-image gather at \mathbf{x} .

By means of Laplace’s method and an asymptotic evaluation of the integral (8), Schleicher and Costa (2009) showed that the result of a multipath summation produces a migrated image that is, at each image point \mathbf{x} , proportional to the migration with stationary velocity value, i.e., the one for which the weight function in integral (8) takes its maximum value, and to the weight factor calculated for this velocity. This analysis implies that the use of a slightly modified weight function, $\tilde{w}(\mathbf{x}, \alpha) = \alpha w(\mathbf{x}, \alpha)$ provides, at each point \mathbf{x} , a second migration result that is proportional to the first one, the factor being the stationary value of the velocity at point \mathbf{x} . Thus, the ratio between the migration results provides this velocity value. This property allows for the determination of a velocity value for all points with a nonzero multi-stack image. A complete velocity model can then be constructed by intelligent smoothing (Schleicher and Costa, 2009).

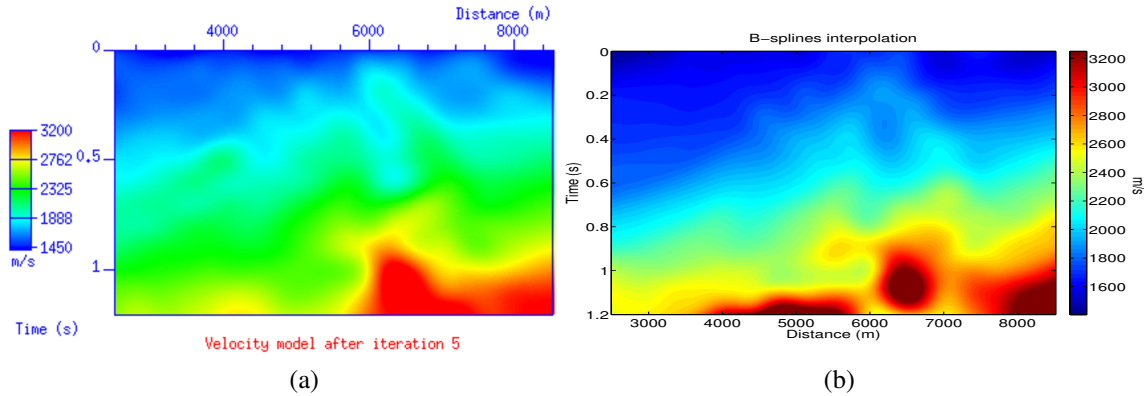


Figure 3: (a) Best time-migration velocity model obtained from MVA (a) after five iterations of image-wave RMO correction (from Schleicher et al., 2008); (b) using the multi-stack migration process (from Schleicher and Costa, 2009).

NUMERICAL EXAMPLES

The process of time imaging needs a smooth velocity model. Both MVA methods by image-wave propagation (Schleicher et al., 2008) and double multi-stack migration (Schleicher and Costa, 2009) provide such a smooth model. Since in the original works, both methods were tested for the Marmousoft model, we can directly compare the results. Comparing the best velocity models obtained by image-wave and double multi-stack MVA, we can see that both image-wave (Figure 3a) and double multi-stack MVA (Figure 3b) produce similar models in the sedimentary parts of the model but yield some visible differences in the geologically complex central part, probably due to the limitations of time migration in such a situation.

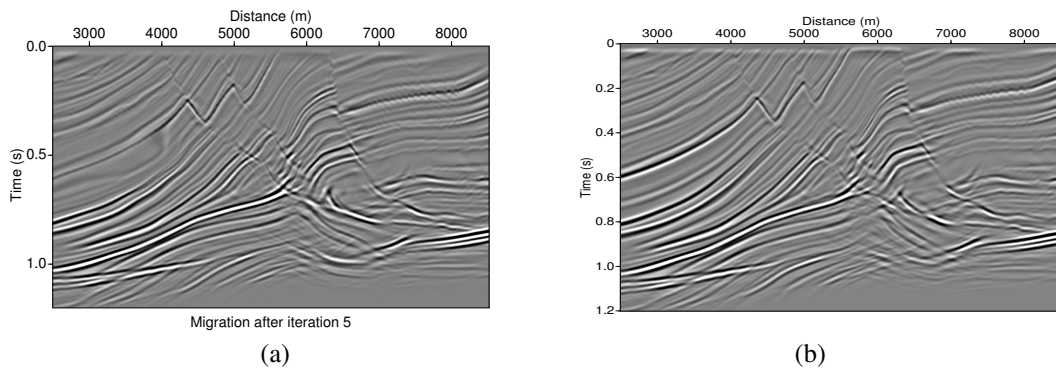


Figure 4: Migrated image obtained by time migration using the velocity model from (a) image-wave RMO correction (from Schleicher et al., 2008); (b) multi-stack migration (from Schleicher and Costa, 2009).

While there is a notable difference between the velocity models, it is not easy to detect important differences in the images resulting from time-migration with these models (Figure 4). This illustrates the ambiguity in the determination of a starting model for more sophisticated iterative methods. Further investigations will need to decide which of the models is better suited for this purpose.

RESULTS

To perform a qualitative and quantitative analysis comparing the result obtained by image-wave propagation of CIGs and double multi-stack migration, we have considered in our analysis:

- the interpolation method applied;
- the number of iterations and computer time required to complete the process;

- and the necessity and duration of human intervention.

Velocity interpolation

Regardless of the method used, a time-migration velocity model must not present abrupt variations. So, when an MVA method generates a grid with blank points, it is necessary to complete these gaps and smooth this velocity model before the migration process can be executed (Schleicher and Costa, 2009). In this regard, linear interpolation can be useful but requires that the data be filtered (e.g., by a moving average) to avoid discontinuities in the velocity derivatives. In our tests, B-splines interpolation turned out to be the best way to interpolate the data, since it smoothed the velocity models even in edge regions. Therefore, all results presented here were obtained using B-splines interpolation.

An important parameter in this process is the number of B-splines nodes for the velocity interpolation. We have tested different grid sizes, but did not find any significant influence on the quality of the results. However, as the number of nodes increases the processing time also increases. For the examples shown below, the number of B-splines nodes along the vertical axis (in vertical time) was 12 and along the horizontal axis (in horizontal distance) 100.

Image continuation

Parameter setup For the image-wave propagation of CIGs, we started in all the tests from a constant velocity model with 1500 m/s (water velocity). The initial and final velocities required for the image-wave propagation technique were set as 1500 m/s and 6500 m/s, respectively. Moreover, to use the migration velocity as the propagation variable in the image continuation, we have to treat the CIGs as if obtained with a constant velocity v_c . The choice of v_c is rather arbitrary because the principle does not depend on its actual value. In practice, it is helpful to avoid too large velocity differences to the background model. Given the range of true velocities in the Marmousoft model, we chose $v_c = 2000$ m/s. From this reference velocity, we continued CIGs to larger velocities up to 3500 m/s and to lower velocities down to 1500 m/s in steps of $\Delta v = 10$ m/s.

Automated velocity picking from propagated CIGs Schleicher et al. (2008) showed that time migration velocity analysis by image-wave propagation of CIGs allows to determine a meaningful velocity model and a migrated image of acceptable quality (Figure 4a). However, to do so, they had to manually pick the flattening velocities, which made the process rather cumbersome.

In this work, we perform the process without any human intervention using two automatic picking procedures. Both consider the semblance values along horizontal lines in the propagated CIGs. The first procedure picks the velocities for all maxima in the semblance panel (Figures 5 and 6), while the second procedure picks the maxima after smoothing (Figures 7 and 8).

The velocity model and its respective migrated image for the third and fifth iteration are depicted, respectively, in Figures 5-7 and Figures 6-8. Our results indicate that already after the third iteration we can produce an acceptable velocity model for the lateral regions where the geology is not so complex (less variation). In the more complex central part of the model, additional improvement is achieved up to the fifth iteration. More iterations of the process led to no further improvement, indicating that the remaining inaccuracies cannot be resolved by time migration.

Computational Cost The largest part of the computation cost of image-wave remigration resides in the migrations necessary at each iteration. The image-wave propagation of the CIGs are about two orders of magnitude faster. In the original implementation of Schleicher et al. (2008), severe human interaction was required (they picked flattening velocities at 95 CIGs in 5 iterations). Here, we tested how automatic picking could be used to accelerate the procedure. The experience was quite positive. Although the automatic picking provides slightly less quality in the extracted velocities, there was no need for more iterations in the automatic process than in the interactive process to achieve a final model of about the same quality.

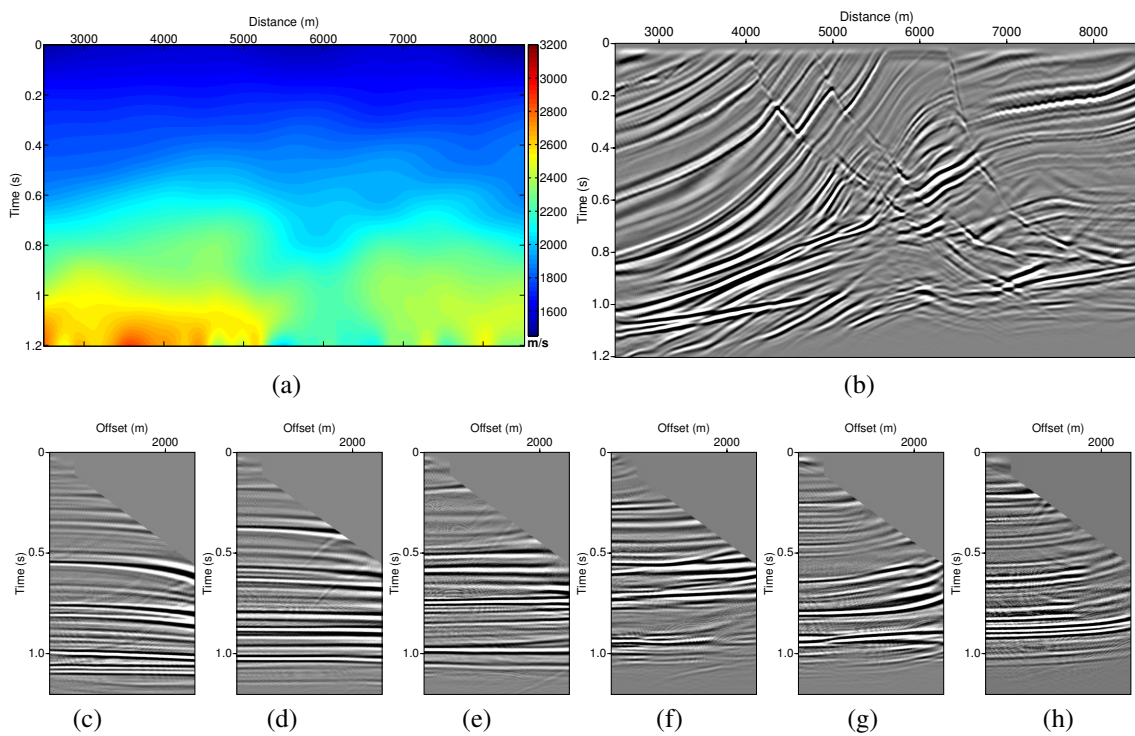


Figure 5: Third iteration of the image-wave propagation method using auto-picks at the maxima of horizontal semblance. Shown are the velocity model (a), the final migrated image (b), and common-image gathers from time migration at (c) 3000 m, (d) 4000 m, (e) 5000 m, (f) 6000 m, (g) 7000 m and (h) 8000 m.

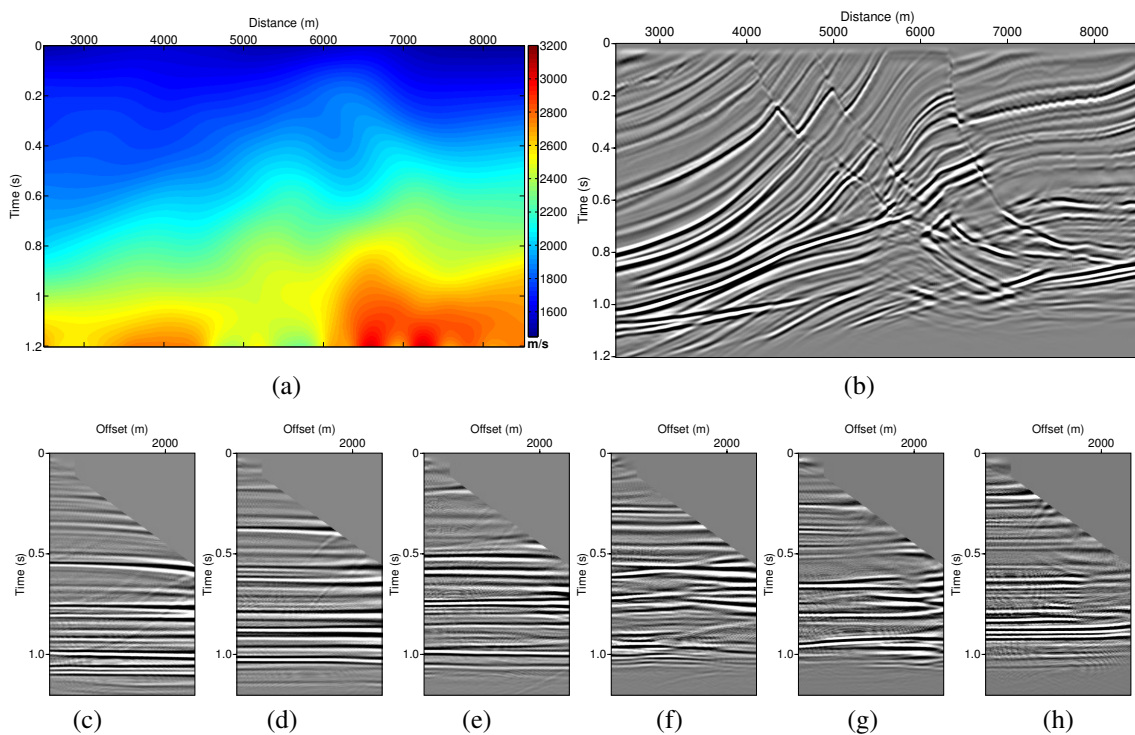


Figure 6: Fifth iteration of the image-wave propagation method using auto-picks at the maxima of horizontal semblance. Shown are the velocity model (a), the final migrated image (b), and common-image gathers from time migration at (c) 3000 m, (d) 4000 m, (e) 5000 m, (f) 6000 m, (g) 7000 m and (h) 8000 m.

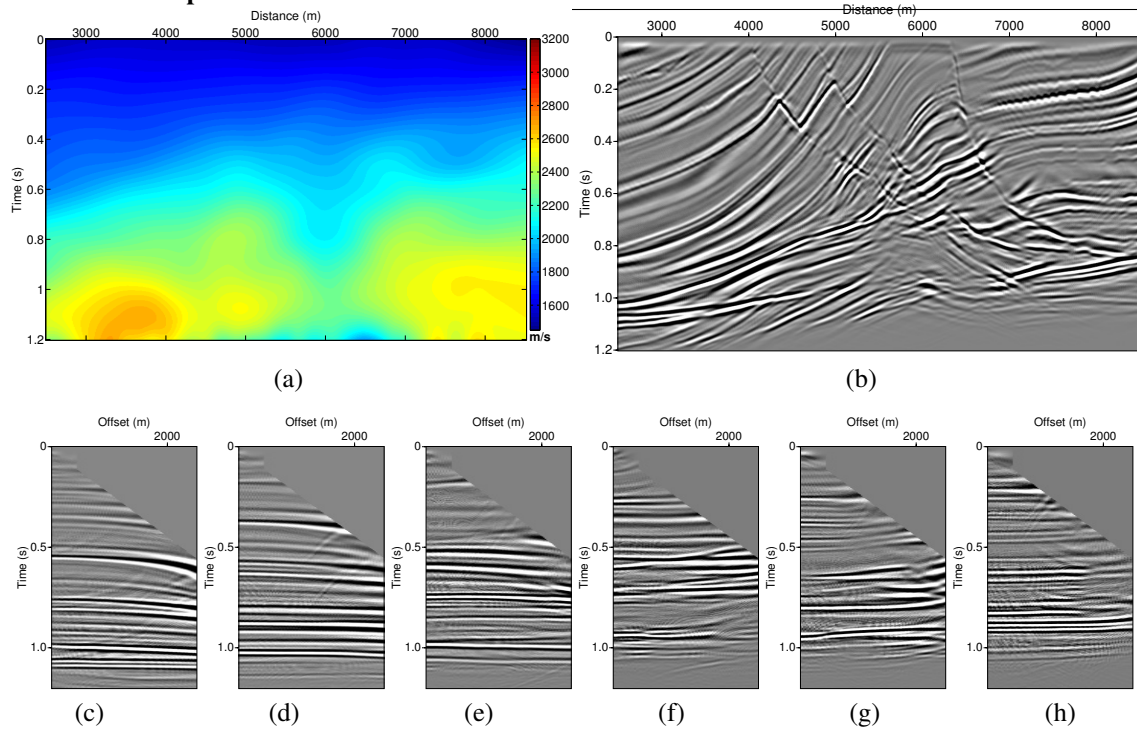


Figure 7: Third iteration of the image-wave propagation method using auto-picks at the maxima of smoothed horizontal semblance. Shown are the velocity model (a), the final migrated image (b), and common-image gathers from time migration at (c) 3000 m, (d) 4000 m, (e) 5000 m, (f) 6000 m, (g) 7000 m and (h) 8000 m.

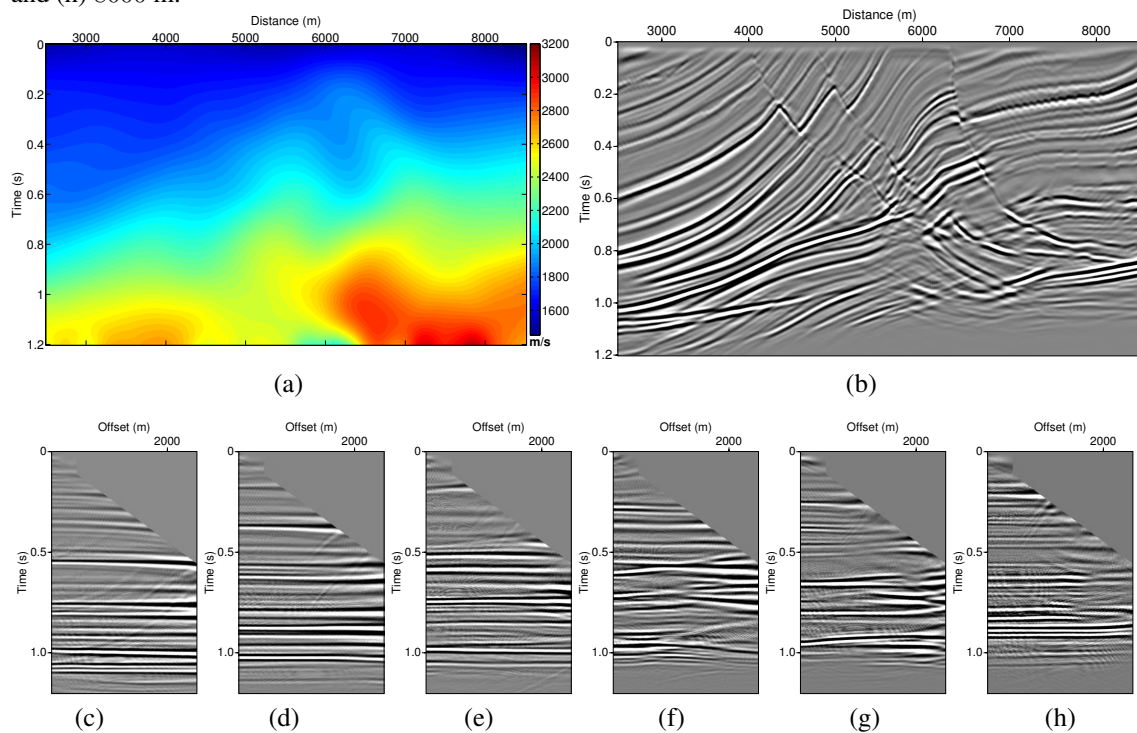


Figure 8: Fifth iteration of the image-wave propagation method using auto-picks at the maxima of smoothed horizontal semblance. Shown are the velocity model (a), the final migrated image (b), and common-image gathers from time migration at (c) 3000 m, (d) 4000 m, (e) 5000 m, (f) 6000 m, (g) 7000 m and (h) 8000 m.

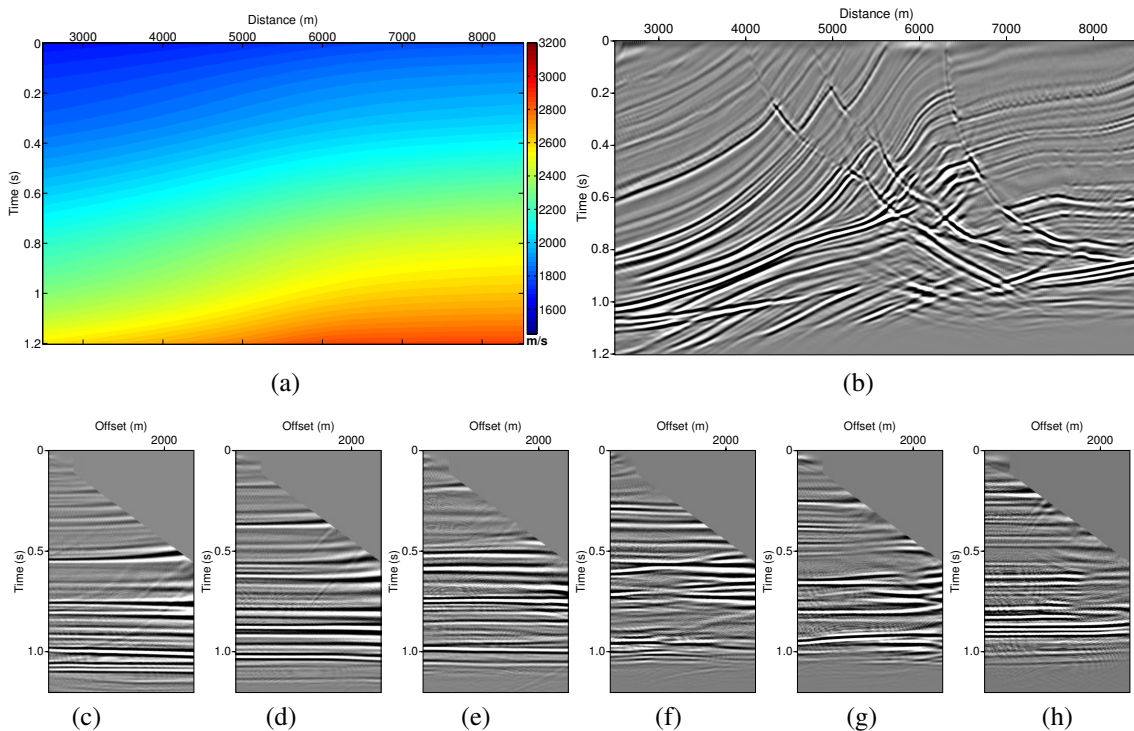


Figure 9: Results of multi-stack MVA with strong regularization. Shown is the velocity model (a); the time-migrated image (b); and common-image gathers from time migration at (c) 3000 m, (d) 4000 m, (e) 5000 m, (f) 6000 m, (g) 7000 m and (h) 8000 m.

Multi-stack migration

Parameter setup The most fundamental parameter in multi-stack migration velocity analysis is the quantity used to measure flatness of an event in a CIG. We use the same parameter as in the original work of Schleicher and Costa (2009), being the sum over the squares of the local slopes along a horizontal line in the CIG.

As in the image-wave propagation of CIGs, the double multi-stack migration needs to scan between a minimum (v_{min}) and maximum (v_{max}) velocity values. The results presented here were obtained setting up $v_{min} = 1400$ m/s and $v_{max} = 4200$ m/s, with a velocity sampling interval $\Delta v = 25$ m/s. These values can be chosen almost arbitrarily as long as the velocity range is large enough to ensure the properties and limitations of the method. It is possible to use a priori information to reduce the number of migrations, for example, discarding unrealistic velocity values.

Regularization Since the method extracts velocity values only at points where the image is nonzero, the B-splines interpolation needs some regularization. This is achieved by a relative weight of each constraint in the cost function (Costa and Schleicher, 2011). The resulting model is rather sensitive to the choice of the regularization parameter. Here, we tested how to choose this parameter in order to arrive at a comparable model to the one from CIG continuation. Figures 9 to 11 show the results of the velocity extraction using double multi-stack migration velocity analysis under three different forms of regularization. Note that the resulting velocity models are considerably different.

Parts a of Figures 9, 10 and 11 show the velocity model computed by a strong, intermediate, and weak regularization, respectively. In comparison with the models of Figures 5 to 8, it is easy to see that the velocity model obtained with a strong regularization (Figure 9) is much smoother. In turn, after weak regularization the model presents too much detail for a time-migration model. Also, boundary effects of the B-splines interpolation start to affect the resulting model. Note the high velocity values in the upper part and low values in the bottom part of the velocity model (Figure 11). The velocity model obtained

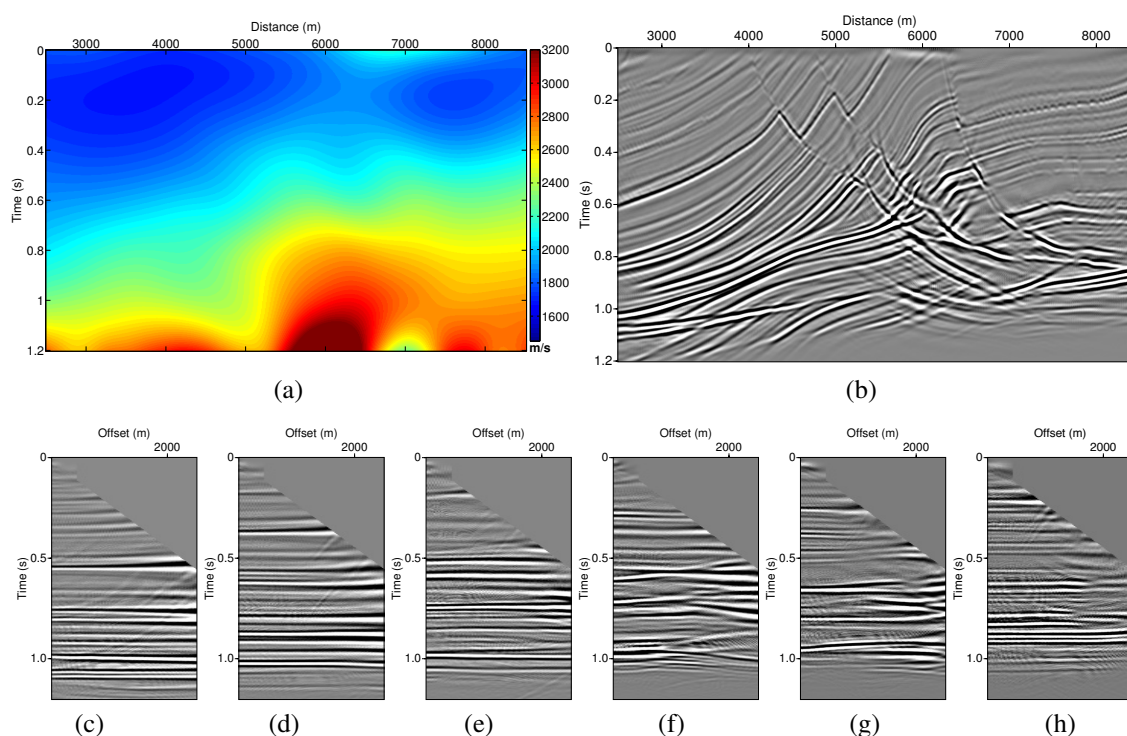


Figure 10: Results of multi-stack MVA with intermediate regularization. Shown is the velocity model (a); the time-migrated image (b); and common-image gathers from time migration at (c) 3000 m, (d) 4000 m, (e) 5000 m, (f) 6000 m, (g) 7000 m and (h) 8000 m.

from an intermediate regularization (Figure 10) seems to be more compatible with the ones obtained by the image-wave propagation of CIGs (Figures 5 to 8).

On the other hand, when we compare the migrated images obtained with these models (parts b of Figures 9, 10 and 11), we see that they are virtually identical. Even in the image gathers (parts c to h), it is hard to spot significant differences. Thus, from an imaging point of view, there is a broad range of regularization that can provide suitable velocity models for an acceptable time-migrated image. Future investigations with subsequent depth conversion will be necessary to decide which level of regularization is most suited in order to find a suitable initial model for depth MVA.

Computational Cost The computational cost of double multi-stack migration is only slightly higher than for a single multi-stack migration. All that is needed is the multiplication of the migrated image by the present velocity, a summation into a second, velocity-weighted image, and a division of the final results at each point in the image. The computationally most expensive part, the time migration for each of the chosen velocities, is done only once. The computational cost of a single multi-stack migration is, of course, N_v times the cost of a single time migration, where N_v is the number of velocities used. However, constant-velocity time migrations are the cheapest possible migrations. Moreover, these time migrations are completely independent of each other, making the process fully parallelizable.

The total cost of the proposed velocity analysis is just the one of double multi-stack migration. The velocity extraction, interpolation, and smoothing can be done fully automatically, without the need of human interpretation or other intervention. This makes it highly advantageous over conventional velocity-analysis techniques which strongly rely on human interaction.

CONCLUSIONS

We have studied the migration-velocity-analysis methods of image-wave common-image-gather continuation (Schleicher et al., 2008) and multi-stack migration (Schleicher and Costa, 2009). Our comparison of

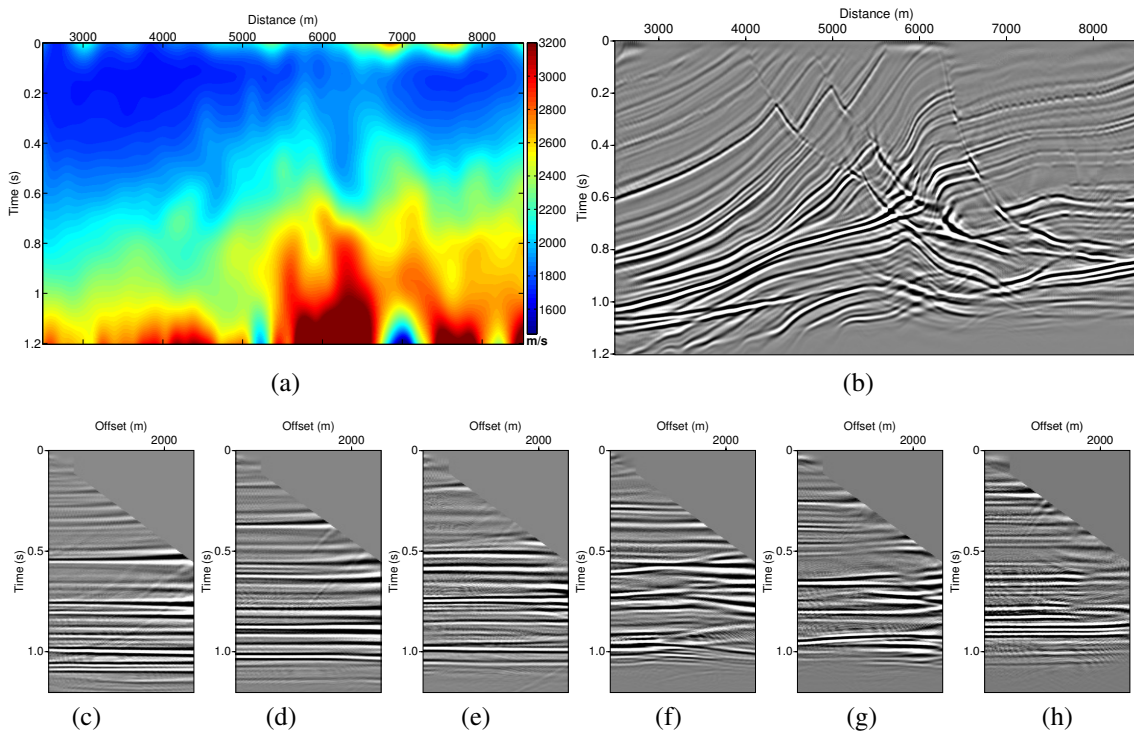


Figure 11: Results of multi-stack MVA with weak regularization. Shown is the velocity model (a); the time-migrated image (b); and common-image gathers from time migration at (c) 3000 m, (d) 4000 m, (e) 5000 m, (f) 6000 m, (g) 7000 m and (h) 8000 m.

the velocity models obtained with both methods revealed that rather different models are obtained depending on the parameterization. However, the associated time-migrated images exhibit fairly much the same quality. This indicates that for the purpose of time-migration, all models are equivalent.

In the original version of (Schleicher et al., 2008), the strongly interactive character of CIG-continuation MVA is a significant drawback. In this paper, we have demonstrated that an automatic implementation of the involved picking of flattening velocities does not degrade the final image or lead to additional iterations. In this way, the technique becomes competitive in terms of computational cost to multi-stack migration MVA, which is completely automatic and exclusively relies on constant-velocity migrations.

We have seen that multi-stack migration MVA can provide a broad range of differently smoothed velocity models. Since in our implementation of CIG-continuation MVA, the velocity model is represented in an identical way, the same should be possible for that method. How a smoother or more detailed model affects the result of the image-wave propagation is a topic of ongoing research.

One difference of the methods is that multi-stack migration allows to extract a velocity model without any a-priori information whatsoever, while the velocity continuation method needs a (fairly arbitrary) initial model. In our applications, starting from a constant-velocity model (e.g., water velocity) was always sufficient to reach a reasonable time-migration velocity model. A fairly intuitive extension of the present research is to use the velocity model generated by multi-stack imaging as an initial model in velocity continuation.

Our evaluation demonstrates that both methods are equivalent regarding the final result, i.e., the time-migrated image. In summary, the methods were shown to be qualitatively and quantitatively consistent. Both of them proved to be capable of calculating a representative velocity model, with their results depending on the choice of some fundamental parameters.

The broad range of obtainable models that produce equivalent image quality in time migration is a strong indicator that the investigated techniques can be employed to construct initial models for a subsequent more sophisticated depth migration-velocity analysis. In order to evaluate which parameterization will lead to the best-suited starting models, a time-to-depth conversion to depth will be necessary to com-

pare the attainable model quality.

ACKNOWLEDGEMENTS

We thank Jadsom de Figueiredo and Douglas Silvestre for their comments and suggestions. The first authors acknowledges support of this research by a fellowship from CGG-Brazil. We are grateful for the financial support from Petrobras, the Brazilian national research agencies CNPq, FAPESP, FINEP, and CAPES, as well as the sponsors of the *Wave Inversion Technology (WIT) Consortium*, Germany.

REFERENCES

- Al-Yahya, K. M. (1989). Velocity analysis by iterative profile migration. *Geophysics*, 54(06):718–729.
- Billette, F., Le Bégat, S., Podvin, P., and Lambaré, G. (2003). Practical aspects and applications of 2D stereotomography. *Geophysics*, 68(3):1008–1021.
- Cameron, M. K., Fomel, S. B., and Sethian, J. A. (2007). Seismic velocity estimation from time migration. *Inverse Problems*, 23:1329–1369.
- Cameron, M. K., Fomel, S. B., and Sethian, J. A. (2008). Time-to-depth conversion and seismic velocity estimation using time-migration velocity. *Geophysics*, 73(5):VE205–VE210.
- Clapp, R. G., Biondi, B., and Claerbout, J. F. (2004). Incorporating geologic information into reflection tomography. *Geophysics*, 69(2):533–546.
- Costa, J. C. and Schleicher, J. (2011). Double path-integral migration velocity analysis: a real data example. *Journal of Geophysics and Engineering*, 8:154–161.
- Fomel, S. (2003). Time migration velocity analysis by velocity continuation. *Geophysics*, 68(5):1662–1672.
- Hertweck, T., Schleicher, J., and Mann, J. (2007). Data stacking beyond CMP. *The Leading Edge*, 26(7):818–827.
- Hubral, P. (1977). Time migration – some ray theoretical aspects. *Geophysical Prospecting*, 25:738–745.
- Iversen, E. and Tygel, M. (2008). Image-ray tracing for joint 3D seismic velocity estimation and time-to-depth conversion. *Geophysics*, 73(3):S99–S114.
- Landa, E., Fomel, S., and Moser, T. J. (2006). Path-integral seismic imaging. *Geophysical Prospecting*, 54(5):491–503.
- Rocca, F. and Salvador, L. (1982). Residual migration. *52nd Annual International Meeting, SEG, Expanded Abstracts*, pages 4–7.
- Schleicher, J. and Biloti, R. (2007). Dip correction for coherence-based time migration velocity analysis. *Geophysics*, 72(1):S431–S48.
- Schleicher, J. and Costa, J. C. (2009). Migration velocity analysis by double path-integral migration. *Geophysics*, 74(6):WCA225–WCA231.
- Schleicher, J., Costa, J. C., and Novais, A. (2008). Time-migration velocity analysis by image-wave propagation of common-image gathers. *Geophysics*, 73(5):VE161–VE171.
- Virieux, J. and Operto, S. (2009). An overview of full-waveform inversion in exploration geophysics. *Geophysics*, 74(6):WCC1–WCC26.